

Research

Open Access

Activation of the SPHK/SIP signalling pathway is coupled to muscarinic receptor-dependent regulation of peripheral airways

Melanie Pfaff¹, Norbert Powaga¹, Sibel Akinci¹, Werner Schütz¹, Yoshiko Banno², Silke Wiegand¹, Wolfgang Kummer¹, Jürgen Wess³ and Rainer Viktor Haberberger*¹

Address: ¹Institute for Anatomy and Cell Biology Justus-Liebig-University Giessen, Germany, ²Department of Cell Signaling, Graduate School of Medicine, Gifu University, Gifu, Japan and ³Laboratory of Bioorganic Chemistry, National Institute of Diabetes and Digestive Kidney Diseases, Bethesda, Maryland 20892, USA

Email: Melanie Pfaff - Mel.pfaff@gmx.de; Norbert Powaga - Norbert.powaga@web.de; Sibel Akinci - Sibel.akinci@web.de; Werner Schütz - Werner-schuetz@web.de; Yoshiko Banno - banno@cc.gifu-u.ac.jp; Silke Wiegand - Silke.wiegand@anatomie.med.uni-giessen.de; Wolfgang Kummer - Wolfgang.kummer@anatomie.med.uni-giessen.de; Jürgen Wess - jwess@helix.nih.gov; Rainer Viktor Haberberger* - Rainer.v.haberberger@anatomie.med.uni-giessen.de

* Corresponding author

Published: 31 May 2005

Received: 12 November 2004

Respiratory Research 2005, **6**:48 doi:10.1186/1465-9921-6-48

Accepted: 31 May 2005

This article is available from: <http://respiratory-research.com/content/6/1/48>

© 2005 Pfaff et al; licensee BioMed Central Ltd.

This is an Open Access article distributed under the terms of the Creative Commons Attribution License (<http://creativecommons.org/licenses/by/2.0>), which permits unrestricted use, distribution, and reproduction in any medium, provided the original work is properly cited.

Abstract

Background: In peripheral airways, acetylcholine induces contraction via activation of muscarinic M₂- and M₃-receptor subtypes (M₂R and M₃R). Cholinergic hypersensitivity is associated with chronic obstructive pulmonary disease and asthma, and therefore the identification of muscarinic signaling pathways are of great therapeutic interest. A pathway that has been shown to be activated via MR and to increase [Ca²⁺]_i includes the activation of sphingosine kinases (SPHK) and the generation of the bioactive sphingolipid sphingosine 1-phosphate (SIP). Whether the SPHK/SIP signaling pathway is integrated in the muscarinic control of peripheral airways is not known.

Methods: To address this issue, we studied precision cut lung slices derived from FVB and M₂R-KO and M₃R-KO mice.

Results: In peripheral airways of FVB, wild-type, and MR-deficient mice, SPHK1 was mainly localized to smooth muscle. Muscarine induced a constriction in all investigated mouse strains which was reduced by inhibition of SPHK using D, L-threo-dihydrosphingosine (DHS) and N, N-dimethyl-sphingosine (DMS) but not by N-acetylsphingosine (N-AcS), a structurally related agent that does not affect SPHK function. The initial phase of constriction was nearly absent in peripheral airways of M₃R-KO mice when SPHK was inhibited by DHS and DMS but was unaffected in M₂R-KO mice. Quantitative RT-PCR revealed that the disruption of the M₂R and M₃R genes had no significant effect on the expression levels of the SPHK1-isoform in peripheral airways.

Conclusion: These results demonstrate that the SPHK/SIP signaling pathway contributes to cholinergic constriction of murine peripheral airways. In addition, our data strongly suggest that SPHK is activated via the M₂R. Given the important role of muscarinic mechanisms in pulmonary disease, these findings should be of considerable therapeutic relevance.

Background

Acetylcholine (ACh), released from parasympathetic nerve fibres, leads to bronchoconstriction via stimulation of muscarinic acetylcholine receptors (MRs) and subsequent increase in intracellular calcium levels $[Ca^{2+}]_i$. The MR-family consists of five molecularly distinct subtypes ($M_{1-5}R$) that are coupled to heterotrimeric G-proteins [1,2]. Activation of the M_2R and M_4R subtypes generally decreases intracellular cAMP levels, whereas stimulation of the M_1R , M_3R and M_5R subtypes leads to the activation of phospholipase C β (PLC β) with subsequent generation of the second messenger inositol 1, 4, 5-trisphosphate (IP $_3$) and an increase in $[Ca^{2+}]_i$ [1,2]. Asthmatic patients show hypersensitivity to MR agonists, and consequently antimuscarinic agents are commonly used in treatment of upper and lower airway diseases [3].

Several studies suggest that the PLC-IP $_3$ -signalling pathway is not solely responsible for changes in $[Ca^{2+}]_i$. For example, activation of the cyclic ADP-ribose pathway abolishes ACh-induced Ca^{2+} oscillations in smooth muscle of porcine airways (White et al. 2003). Another alternative pathway that has been shown to increase $[Ca^{2+}]_i$ involves the activation of sphingosine kinases (SPHK) and the subsequent generation of the bioactive sphingolipid sphingosine 1-phosphate (S1P) [4-6]. While S1P is well known as an important extracellular mediator of many biological pathways, including cell survival, angiogenesis and cell migration, recent studies indicate that S1P is also an intracellular second messenger which is coupled to changes in intracellular Ca^{2+} levels [4-6]. In the airways, S1P has been shown to stimulate airway smooth muscle proliferation and cytokine release [7]. When applied to cultured human tracheal myocytes, S1P also increases $[Ca^{2+}]_i$ and evokes contractile responses [7,8]. Moreover, muscarinic activation of M_2R - and M_3R -transfected HEK293 cells stimulates S1P synthesis [4,5]. In the present study we therefore tested the hypothesis that activation of the SPHK/S1P signalling pathway may contribute to MR-dependent regulation of peripheral airway diameter. For all studies we used airways from wild-type (wt) and M_2R and M_3R mutant mice that were ~ 200 μm in diameter. It is well known that smaller airways are mainly responsible for airway resistance [9,10]. Moreover previous studies clearly demonstrated differences between larger and smaller airways concerning functional responses, receptor expression or ion conductance [11].

In murine tissues, S1P is synthesized after activation of two SPHK isoforms, SPHK1 and SPHK2. SPHK1 is highly expressed in adult lung [12-14], whereas the SPHK2 isoform shows much lower expression in lung tissue [15]. SPHK2 contains a nuclear localization sequence and has recently been identified as a nuclear protein capable of inhibiting DNA synthesis, whereas SPHK1 is mainly local-

ized in the cytosol [14,16]. In the present study we therefore focused exclusively on the expression and potential functional role of the SPHK1 isoform in MR-mediated airway constriction.

The expression of the SPHK1 isoform was investigated by means of quantitative RT-PCR and immunohistochemistry using precision cut lung slices (PCLS) of murine lungs [17]. Using murine PCLS we also measured the constriction of small intraparenchymal airways in response to MR activation. Coupling of MRs to SPHK-activation was investigated by blocking SPHK with D, L-threo-dihydrosphingosine (DHS) or N, N-dimethyl-sphingosine (DMS, [18]). Moreover, the role of MR-dependent intracellular Ca^{2+} release on airway diameter was studied by inhibiting Ca^{2+} -influx by La^{3+} and SKF 96365. Recent evidence indicates that MR agonists induce bronchoconstriction by activating a mixture of M_2R and M_3R subtypes, present on smooth muscle cells of extra- and intraparenchymal airways [19,20]. To study the potential roles of the M_2R and M_3R subtypes in SPHK1-dependent peripheral airway responses, we therefore also carried out functional studies with PCLS prepared from M_2R - and M_3R -deficient mice (M_2R -KO, M_3R -KO) and their corresponding wild type controls (M_2R -wt, M_3R -wt) [21,22].

Methods

Animals

Lungs were taken from 8-12 wk old FVB mice (Harlan-Winkelmann, Borcheln, Germany), mice deficient in M_2R or M_3R (M_2R -KO, M_3R -KO) and their corresponding wild-type strains (M_2R -wt, M_3R -wt). The generation of M_2R -KO and M_3R -KO mice has been described previously [21,22]. The M_2R -KO mice and the M_2R -wt mice had the following genetic background: 129J1 (50%) \times CF1 (50%). The M_3R -KO mice and the corresponding wild-type mice had the following genetic background: 129SvEv (50%) \times CF1 (50%). The animals were killed by cervical dislocation. The mice were kept under specific pathogen free conditions until the experiments.

Quantitative RT-PCR

Real-time quantitative PCR (iCycler, Bio-Rad, Munchen, Germany) was used to quantify levels of SPHK1 mRNA in PCLS of FVB, M_2R -KO, M_3R -KO, M_2R -wt, and M_3R -wt mice. Lung slices were transferred into lysis buffer (Qiagen, Heiden, Germany) and homogenized using a mixer mill with a frequency of 300 Hz (Qiagen). Total RNA was isolated according to the protocol recommended by the manufacturer (Rneasy kit, Qiagen). Contaminating DNA was removed using DNase (1 U/ μg total RNA, Gibco-BRL, Life Technologies, Karlsruhe, Germany) in the presence of 20 mM Tris-HCl (pH 8.4), 2 mM $MgCl_2$, 50 mM KCl for 15 min at 25°C. Equal amounts of RNA were reverse transcribed in the presence of 3 mM $MgCl_2$, 75 mM KCl, 50

mM Tris-HCl (pH 8.3), 10 mM dithiothreitol, 0.5 mM dNTPs (Gibco-BRL) and 25 µg oligo (dT) (MWG Biotech, Ebersberg, Germany), with 200 U of Superscript RNase H-Reverse transcriptase (Gibco-BRL) for 50 min at 42°C. Gene specific PCR primers for mouse SPHK1 and β_2 -microglobulin (SPHK1, gi:22094104, fw TCCAGAAACCCCTGTGTAGC, rev GCTCCCTAGGGCCAGTAAAC product size 188 bp, β_2 -microglobulin gi:12861272 fw ATGGGAAGCCGAACATACTG, rev CAGTCTCAGTGGGGTGAAT, product size 176 bp) were designed using Primer Express™ software (Applied Biosystems, Foster City, USA). All PCR-reactions were prepared in triplicate from four to eight animals using a ready-to-use kit according to the manufacturers protocol (QuantiTect™ SYBR Green PCR Kit, Qiagen). Primers specific for β -microglobulin were used for standardisation. The data were normalised by subtracting the threshold cycle (CT) levels between SPHK1 and β_2 -microglobulin. In each independent experiment qRT-PCR reactions were performed in triplicate.

Double-labelling immunofluorescence

Slices (220 µm thick) prepared for videomorphometry were fixed for 20 min in ice-cold acetone and washed repeatedly in 0.1 M phosphate buffer. Sections were covered for 1 h with blocking medium (50 % normal porcine serum in PBS) followed by overnight incubation with an antiserum directed against the SPHK1 isoform (1:400, [23]) in combination with a monoclonal FITC-labelled anti- α -smooth muscle actin antibody (1:500, clone 1A4, Sigma, Deisenhofen, Germany). The sections were then washed in PBS and covered for 1 h with Cy3-conjugated donkey anti-rabbit Ig antiserum (1:3000, Dianova, Hamburg, Germany). After incubation with the secondary antibody, the slides were washed in PBS and coverslipped in carbonate-buffered glycerol at pH 8.6. Omission of primary antisera or preabsorption of the SPHK1a antiserum with the corresponding synthetic peptide (20–100 µg antigen/ml diluted antiserum) abolished immunolabelling. The slides were evaluated by sequential confocal laser scanning microscopy (TCPS, Leica, Bensheim, Germany) using the appropriate laser for Cy3 (excitation 543 nm) and FITC (excitation 488 nm).

Videomorphometry

PCLS were prepared using a slightly modified version of the protocol described by Martin et al. [24]. Briefly, the mice were killed by cervical dislocation and the lungs were perfused via the right ventricle with 37°C Krebs-Ringer buffer containing heparin (1000 I.U.), penicillin/streptomycin (1 %) and sodium nitroprusside (0.075 µM). The airways were filled via the cannulated trachea with agarose (low melting point agarose, 1.6 % in Krebs-Ringer buffer, Sigma, Deisenhofen, Germany). Subsequently, the lungs and heart were removed *en bloc*, placed in ice-cold HEPES-

Ringer buffer and cut in 200–250 µm thick slices using a vibratome (VT1000S, Leica). Subsequently, the precision cut lung slices (PCLS) were incubated in minimal essential medium (MEM) at 37°C for 4–7 h. Experiments were performed in a lung slice superfusion chamber (Hugo Sachs Elektronik, March, Germany) mounted on an inverted microscope (Leica). Images were recorded using a CCD-camera (Stemmer Imaging, Puchheim, Germany) and analyzed using the Optimas 6.5 image analysis software (Stemmer). The slices were fixed in the chamber with nylon strings that were connected to a platinum ring. Viable airways of about 200 µm in diameter were examined and incubated in the slide chamber for 5 min in HEPES-Ringer buffer until the first image was acquired. The area of the airway lumen at the beginning of the experiment was defined as 100 % and bronchoconstriction or dilatation were expressed as relative decrease or increase of this area. Data from FVB mice and wt-strains were used only from those experiments where the reduction of luminal area in response to 10^{-6} M muscarine reached at least 25 %. Muscarine, [propoxy]-ethyl-1H-imidazole] (SKF96365), lanthanum chloride and N-acetylsphingosine (N-AcS) were purchased from Sigma. D, L-threo-dihydrosphingosine (DHS) and N,N-dimethyl-sphingosine (DMS) were purchased from Biomol (Hamburg, Germany).

Statistical analysis

Data are presented as means \pm standard error of the mean (SEM) of 5–10 slices obtained from five to nine animals. Matched pairs were evaluated by Wilcoxon's rank sum test. In the case of more than 2 non-matched groups, Mann-Whitney U-test for comparison between two groups was conducted only when statistically significant differences were reached by the global Kruskal-Wallis test that was performed first. Differences were considered as statistically significant when $p < 0.05$.

Results

The goal of the present study was to determine the potential involvement of SPHK1 activation in the MR-mediated constriction of small peripheral airways. To be able to measure the diameter of small murine airways, we used videomicroscopy of viable precision-cut lung slices (PCLS; [24,20]). Specifically, we analyzed the effects of SPHK1 blockade in FVB and M_2R and M_3R single-knock-out mice (M_2R -KO and M_3R -KO mice, respectively) as well as the corresponding wild-type control animals (M_2R -wt and M_3R -wt mice, respectively).

qRT-PCR

We used qRT-PCR analysis to quantitate and compare SPHK1-mRNA levels between FVB mice, M_2R - and M_3R -deficient mice (M_2R -KO, M_3R -KO), and the corresponding wt control mice (M_2R -wt, M_3R -wt). Expression of β_2 -

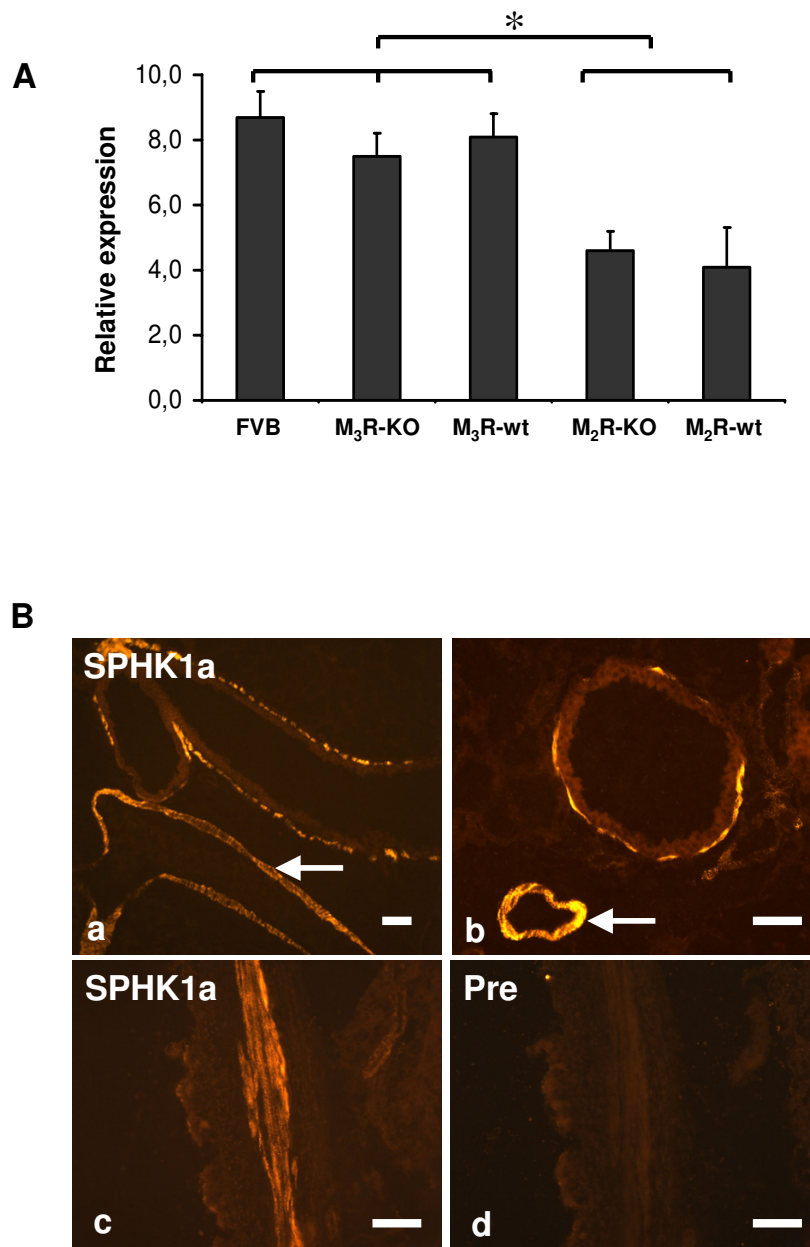


Figure 1

A) Quantitative RT-PCR analysis of SPHK1 expression in PCLS from different mouse strains. The relative expression of SPHK1-mRNA in relation to the house-keeping gene β_2 microglobulin is shown. Data are given as means \pm S.E.M. of four independent experiments each carried out in triplicate. B) Indirect immunofluorescence studies examining SPHK1 expression in PCLS of FVB-mice. Immunoreactivity for SPHK1 was present in the wall of larger (a) and smaller (b) airways and in the media of pulmonary vessels (arrows in a, b). Consecutive sections (c, d) showing that preabsorption of the SPHK1 antiserum abolished immunolabelling (Pre, d). Bars = 50 μ m.

microglobulin served as an internal control. We found that inactivation of the M_2R and M_3R genes had no significant effect on the relative expression levels of SPHK1 compared to their corresponding wt controls (Mann-Whitney U-test, Fig. 1A). This analysis also showed that SPHK1 expression was significantly lower in M_2R -wt and M_2R -KO mice, as compared to FVB, M_3R -wt, and M_3R -KO-mice ($p < 0.05$, Mann-Whitney U-test, Fig. 1A), perhaps due to the fact that the M_2R -KO/wt mice have a genetic background that is somewhat different from that of the other mice used (for details see "Materials and Methods").

Immunohistochemistry

We used single-and double-labeling immunohistochemistry to examine the distribution of SPHK1 in murine peripheral lung. Strong SPHK1-immunoreactivity was detected in the smooth muscle cells of intraparenchymal bronchi (Figs. 1B, 2) and pulmonary arteries (Fig. 1B) and veins as confirmed by double-staining of a marker of smooth muscle cells, α -smooth muscle actin. Preabsorption of the SPHK1 antiserum abolished immunolabelling (Fig. 1B). Immunoreactivity for SPHK1 was absent in bronchial epithelium (Figs. 1B, 2). SPHK1 showed a granular cytoplasmic localisation but was also found in smooth muscle membranes (Fig. 2). The pattern of SPHK1 immunoreactivity was very similar in PCLS of FVB, M_2R -KO/wt, and M_3R -KO/wt mice..

Videomorphometry

FVB mice In PCLS preparations from FVB mice, the luminal area of peripheral bronchi rapidly decreased within the first 2 minutes after application of 10^{-6} M muscarine, followed by a sustained decrease in presence of the agonist (Tab. 1, Fig. 3). Application of the SPHK inhibitors DMS and DHS alone for ten minutes prior to coadministration of 10^{-6} M muscarine had no significant effect on bronchial luminal diameter (Figs. 3A, B, 5A-D). Coadministration of 10^{-6} M muscarine with DHS (10^{-4} M- 10^{-10} M) significantly reduced both the initial and the sustained phase of the muscarine induced bronchoconstriction (Tab. 1, Fig. 3B). Similarly, coadministration of 10^{-6} M muscarine with 10^{-6} - 10^{-10} M DMS reduced both phases of the muscarine response. However 10^{-4} M DHS had no effect (Tab. 1). Coadministration of 10^{-6} M muscarine with the structurally related sphingolipid N-acetylphingosine (10^{-6} - 10^{-10} M) which has no effect on SPHK1 function [5] did not alter the muscarine induced constriction (Tab. 1).

Inhibition of Ca^{2+} entry by La^{3+} (10^{-6} M) considerably reduced the initial and strongly inhibited the sustained constriction of peripheral airways following the administration of 10^{-6} M muscarine (Tab. 2, Fig. 4A, E, G). Combination of 10^{-8} M DHS or 10^{-8} M DMS with La^{3+} (10^{-6} M) almost completely abolished the initial and the sustained

phase of the muscarine-dependent bronchoconstriction (Tab. 2, Fig. 4C, E, G). The combination of DHS or DMS with La^{3+} further significantly reduced both phases compared to La^{3+} alone (Wilcoxon's rank sum test $p < 0.05$)

Blockade of Ca^{2+} -entry by SKF96365 (10^{-5} M), which inhibits G-protein activated and voltage gated Ca^{2+} -channels, greatly reduced both the initial and the sustained phase of muscarine-induced bronchoconstriction (Tab. 3, Fig. 4B, F, H). Combination of SKF96365 (10^{-5} M) with 10^{-8} M DMS or 10^{-8} M DHS exerted no further reduction of luminal airway area (Wilcoxon's rank sum test, Tab. 2, Fig. 4F, H).

M_2R -KO/wt mice Muscarine (10^{-6} M) stimulation of PCLS preparations from M_2R -KO mice resulted in an initial constriction response that was followed by a slight relaxation (4-8 % relaxation of luminal airway area within 3-15 min, 28 slices/27 lungs, Tab. 3, Fig. 5A, B). In contrast, in PCLS preparations from the corresponding wt mice (M_2R -wt), the initial bronchoconstriction was followed by a sustained constriction response. In PCLS of M_2R -KO and M_2R -wt mice, DHS and DMS (10^{-8} M each) significantly inhibited the initial and sustained phase of muscarine induced constriction (Tab. 3, Fig. 5A, B). The initial constriction was inhibited by about 54 % (luminal area of M_2R -wt: 48 ± 11.5 %; M_2R -KO: 61.5 ± 9.5 %, Tab. 3, Fig. 5A, B) and the sustained phase by about 50 % (luminal area of M_2R -wt: 34 ± 12 %; M_2R -KO: 67.5 ± 15 %, Tab. 3, Fig. 5A, B). The degree of inhibition of the initial phase was comparable between M_2R -wt and M_2R -KO mice.

M_3R -KO/wt mice As in all other experiments, the area of the airway lumen at the beginning of the experiment was defined as 100 %. Application of 10^{-6} M muscarine constricted peripheral airways in wt-mice by about 66 % (28 slices/25 lungs), whereas in M_3R -KO mice the constriction was reduced by about 57 % (29 slices/28 lungs, Tab. 4 Figs. 5C, D, 6). In wt-bronchi, inhibition of SPHK by DHS or DMS (10^{-8} M each) significantly reduced the initial phase of constriction by about 50 % (58 ± 12 %, Tab. 4, Figs. 5C, D, 6). Strikingly, treatment of PCLS from M_3R -KO mice with DHS (10^{-8} M) or DMS (10^{-6} and 10^{-8} M) almost completely abolished the initial constriction response (94 ± 4 %, Tab. 4, Figs. 5, 6). Inhibition of SPHK by DHS (10^{-8} M) or DMS (10^{-6} and 10^{-8} M) significantly reduced the sustained phase of constriction to a comparable degree in M_3R -wt and M_3R -KO mice (Tab. 4, Figs. 5C, D, 6).

Discussion

MR signaling pathways play a key role in the regulation of airway resistance which is determined largely by the diameter of smaller, intrapulmonary airways [25]. A better understanding of the different pathways underlying MR

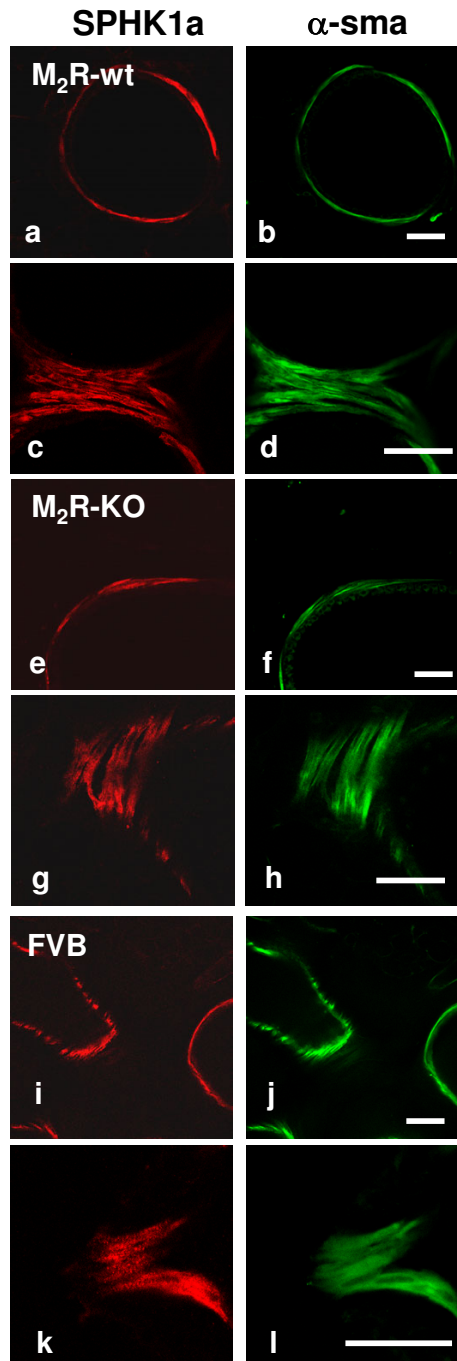


Figure 2

Expression of SPHK1 in PCLS from different mouse strains studied via confocal laser scanning microscopy. Representative confocal laser scanning micrographs of double labeling immunohistochemistry demonstrates the restriction of SPHK1-immunoreactivity to smooth muscle cells, identified by immunoreactivity for the marker protein α -smooth muscle actin (α -sma). SPHK1a-immunoreactivity was present in peripheral airway smooth muscle of knock-out animals (M₂R-KO, a-d) and wild-type (M₂R-wt, e-h, FVB, i-l). Granular immunoreactivity could be detected in the cytoplasm and in the membrane of smooth muscle cells. Bars = 50 μ m

Table 1: Effects of N-AcS, DHS and DMS on muscarine-induced reductions in luminal airway area in FVB mice. The number of experiments (lungs/slices), mean airway diameter in μm , and the luminal airway area determined 1 min (1) and 15 min (2) after stimulation with muscarine (Mus) and 1 min (3) and 15 min (4) after repeated stimulation with muscarine or after repeated stimulation with muscarine in combination with N-AcS, DHS or DMS are shown. In all experiments, the muscarine concentration was 10^{-6} M. Data are given as means \pm S.E.M. Matched pairs (1 vs. 3; 2 vs. 4) were evaluated by Wilcoxon's rank sum test. Differences were considered as statistically significant when $p < 0.05$ (n.s., not significant).

Lungs /slices	Diameter [μm]	Area [%] 1	Area [%] 2	Area [%] 3	Area [%] 4	p (1 vs. 3)	p (2 vs. 4)
			Mus		Mus	n.s.	n.s.
4/4	206 \pm 7	31 \pm 6	38 \pm 4	38 \pm 7	28 \pm 3		
			Mus		Mus/N-AcS 10^{-6} M	n.s.	n.s.
6/5	182 \pm 7	47 \pm 8	42 \pm 8	50 \pm 8	42 \pm 9		
			Mus		Mus/N-AcS 10^{-8} M	n.s.	n.s.
5/5	218 \pm 5	36 \pm 1	28 \pm 5	38 \pm 6	26 \pm 6		
			Mus		Mus/N-AcS 10^{-10} M	n.s.	n.s.
4/4	212 \pm 22	21 \pm 8	16 \pm 5	26 \pm 6	30 \pm 5		
			Mus		Mus/DHS 10^{-4} M	n.s.	n.s.
4/6	194 \pm 9	42 \pm 5	37 \pm 7	61 \pm 8	45 \pm 6		
			Mus		Mus/DHS 10^{-6} M	$p < 0.05$	$p < 0.05$
7/7	197 \pm 14	45 \pm 11	31 \pm 7	70 \pm 13	50 \pm 5		
			Mus		Mus/DHS 10^{-8} M	$p < 0.05$	$p < 0.05$
7/9	181 \pm 6	39 \pm 7	29 \pm 6	50 \pm 9	47 \pm 7		
			Mus		Mus/DHS 10^{-10} M	$p < 0.05$	$p < 0.05$
4/8	198 \pm 6	34 \pm 3	24 \pm 3	42 \pm 4	40 \pm 4		
			Mus		Mus/DMS 10^{-4} M	$p < 0.05$	$p < 0.05$
4/7	180 \pm 7	30 \pm 7	25 \pm 6	45 \pm 10	41 \pm 7		
			Mus		Mus/DMS 10^{-6} M	$p < 0.05$	$p < 0.05$
4/7	201 \pm 11	48 \pm 7	35 \pm 8	70 \pm 6	54 \pm 9		
			Mus		Mus/DMS 10^{-8} M	$p < 0.05$	$p < 0.05$
4/7	206 \pm 11	31 \pm 5	25 \pm 4	54 \pm 8	50 \pm 5		
			Mus		Mus/DMS 10^{-10} M	$p < 0.05$	$p < 0.05$
4/6	196 \pm 15	43 \pm 6	23 \pm 4	71 \pm 11	52 \pm 7		

activation in the intrapulmonary airways is of considerable clinical relevance. In the present study, we examined the hypothesis that S1P might be involved in the muscarinic control of peripheral airways. To address this question, we used the PCLS model which has been shown to maintain the integrity of all components of the peripheral lung including viable peripheral airways [20].

Using double labelling immunohistochemistry we demonstrated for the first time that the SPHK1 protein is highly expressed in the cytosol of murine airway smooth muscle cells with virtually no immunoreactivity in non-smooth muscle cells. On the other hand, human and murine lung tissue showed a high expression and activity of SPHK which was not restricted to smooth muscle alone [13,14]. The virtual restriction of SPHK1-immunoreactivity to smooth muscle could be due to the presence of SPHK isoforms other than SPHK1 in murine lung [14]. At the subcellular level, SPHK1 showed a cytoplasmic localisation but was also found in airway smooth muscle membranes, in agreement with functional and immunoprecipitation studies of mouse lung membranes [14].

In the present study, the use of membrane-permeable SPHK inhibitors, DHS and DMS [18], convincingly demonstrated that MR-mediated constriction of peripheral airways involves the activation of SPHK. In PCLS preparations from wt-mice, both SPHK inhibitors significantly reduced the fast initial constriction response (induced by 10^{-6} M muscarine) which is mainly dependent on Ca^{2+} -release from intracellular stores [26]. This effect was observed with the lowest concentrations of the inhibitors but was absent when DHS and DMS were given alone for ten minutes prior to the application of DHS and DMS in combination with muscarine. This inhibition of muscarine induced bronchoconstriction was also absent when we used N-acetylsphingosine (N-AcS), an agent that is structurally related to DHS and DMS but that does not affect SPHK function [5]. These data suggest that DHS and DMS did not exert their inhibitory effects through non-specific actions. Accordingly, the muscarine-induced initial bronchoconstriction was partly inhibited but persisted in presence of the blockers of Ca^{2+} -influx, La^{3+} or SKF 96365 [27,28], but was almost abolished when La^{3+} was applied in combination with DHS or DMS. The sustained phase of muscarine-induced bronchoconstriction

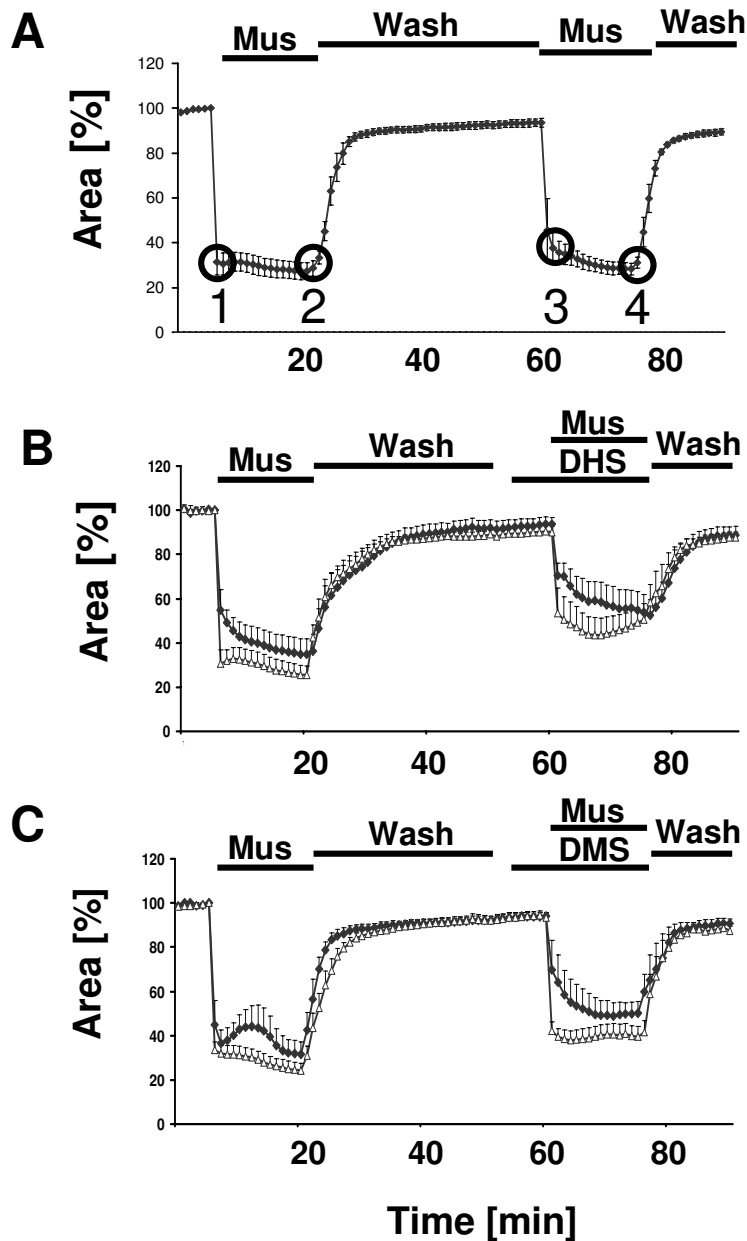


Figure 3

Muscarine-induced reductions in luminal area of peripheral bronchi from FVB mice. (A) Luminal area of peripheral bronchi after application of 10^{-6} M muscarine (Mus) as recorded by videomorphometry. Data (means \pm S.E.M) were expressed as % luminal area. Bronchi from FVB mice (4 slices from 6 lungs) responded to 10^{-6} M muscarine until wash out (Wash). Time points 1–4 were chosen as indicators for initial and sustained constriction. 1 = luminal airway area 1 min after muscarine application, 2 = luminal airway area 15 min after muscarine application, 3 = luminal airway area 1 min after repeated muscarine application, 4 = luminal airway area 15 min after repeated muscarine application. Effect of DHS (B) and DMS (C) on muscarine-mediated reductions in luminal area of peripheral bronchi from FVB mice. The luminal area of peripheral bronchi (expressed in %) was recorded by videomorphometry after application of 10^{-6} M muscarine (Mus) alone and after application of 10^{-6} M muscarine together with (B) 10^{-6} M DHS (diamonds, 7 slices from 4 lungs) and 10^{-10} M DHS (triangles, 8 slices from 4 lungs) or (C) 10^{-6} M DMS (diamonds, 9 slices from 7 lungs) and 10^{-10} M DMS (triangles, 6 slices from 4 lungs). Bronchoconstriction responses were significantly reduced in the presence of DHS and DMS. The inhibition was more pronounced following coadministration of DMS. Data are given as means \pm S.E.M.

Table 2: Effects of SKF96365 and La³⁺ alone and in combination with DHS or DMS on the muscarine-induced reductions in luminal airway area in FVB mice Effects of the Ca²⁺-entry inhibitors La³⁺ (10⁻⁶ M) and SKF 96365 (10⁻⁵ M) alone and in combination with DHS or DMS (both 10⁻⁶ M) on the muscarine induced reduction in luminal airway area (expressed in %). The number of experiments (lungs/slices), mean airway diameter in μ m, and the luminal airway area determined 1 min (1) and 15 min (2) after stimulation with muscarine and 1 min (3) and 15 min (4) and after stimulation with muscarine (Mus) in combination with La³⁺ (Mus/La³⁺) or SKF96365 (Mus/SKF), or after stimulation with muscarine and La³⁺ or SKF96365 in combination with DHS or DMS are shown. In all experiments, the muscarine concentration was 10⁻⁶ M. Data are given as means \pm S.E.M. Matched pairs (1 vs. 3; 2 vs. 4) were evaluated by Wilcoxon's rank sum test. Differences were considered as statistically significant when $p < 0.05$.

Lungs /slices	Diameter [μ m]	Area [%] 1	Area [%] 2	Area [%] 3	Area [%] 4	p (1 vs. 3)	p (2 vs. 4)
4/9	212 \pm 3	Mus 60 \pm 7	Mus 49 \pm 7	Mus/SKF 76 \pm 7	Mus/SKF 86 \pm 3	$p < 0.05$	$p < 0.05$
4/8	193 \pm 12	Mus 51 \pm 5	Mus 43 \pm 6	Mus/SKF/DHS 82 \pm 6	Mus/SKF/DHS 86 \pm 3	$p < 0.05$	$p < 0.05$
5/6	207 \pm 11	Mus 65 \pm 3	Mus 53 \pm 6	Mus/SKF/DMS 88 \pm 2	Mus/SKF/DMS 85 \pm 8	$p < 0.05$	$p < 0.05$
4/7	180 \pm 8	Mus 39 \pm 8	Mus 49 \pm 12	Mus/La ³⁺ 65 \pm 7	Mus/La ³⁺ 89 \pm 2	$p < 0.05$	$p < 0.05$
4/7	211 \pm 12	Mus 40 \pm 4	Mus 33 \pm 3	Mus/La ³⁺ /DHS 85 \pm 2	Mus/La ³⁺ /DHS 89 \pm 2	$p < 0.05$	$p < 0.05$
4/5	210 \pm 15	Mus 45 \pm 9	Mus 38 \pm 9	Mus/La ³⁺ /DMS 94 \pm 2	Mus/La ³⁺ /DMS 95 \pm 1	$p < 0.05$	$p < 0.05$

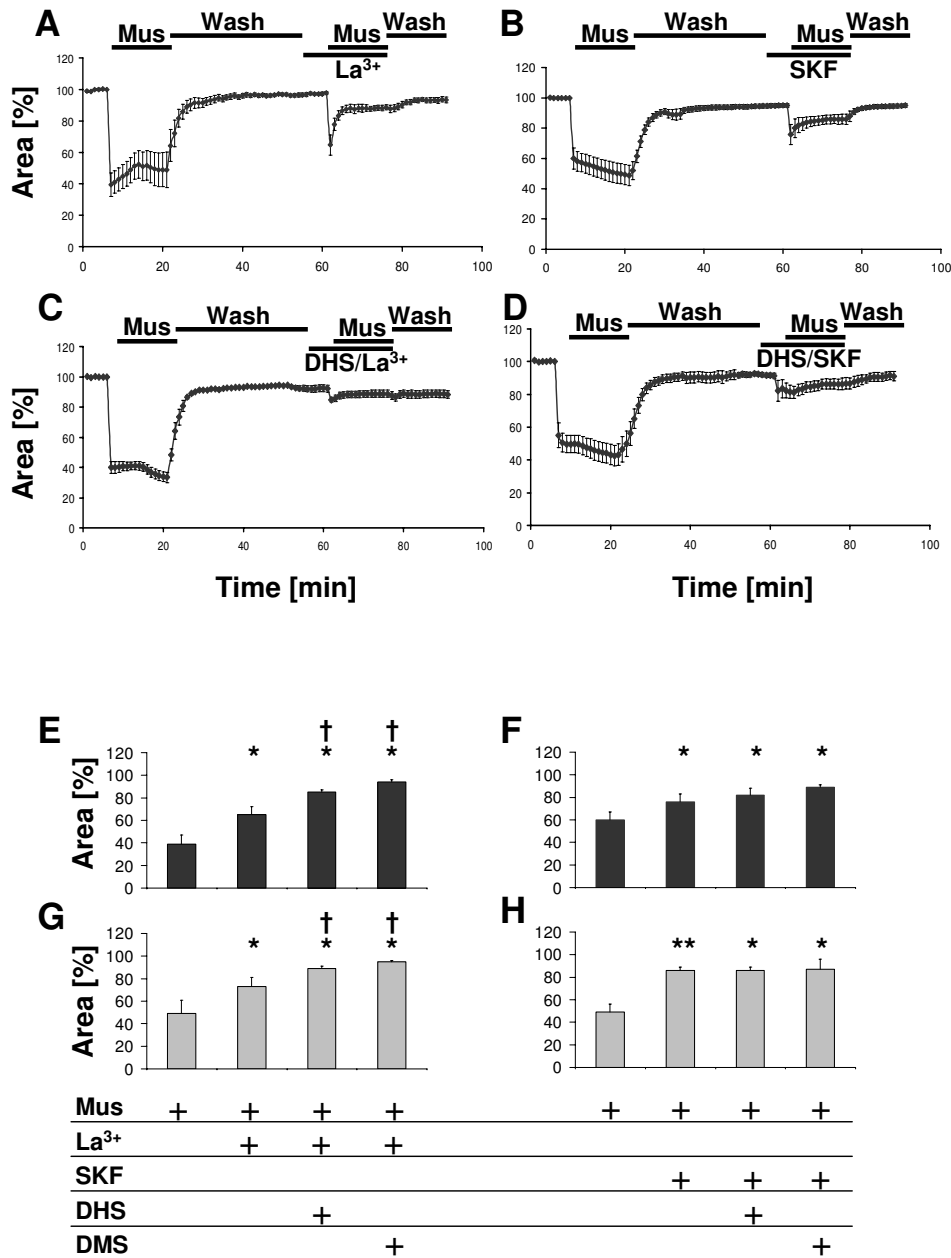
was also significantly inhibited by DHS and DMS in FVB mice. Interestingly, the responses that were inhibited by DHS/DMS were SKF96365-but not La³⁺-sensitive, since DHS/DMS significantly increased the La³⁺-mediated inhibition of the muscarine-mediated constriction, but had no effect on the SKF96365-mediated inhibition of the constriction.

MR-mediated constriction of peripheral airways has been shown to be mediated by a mixture of M₂R and M₃R subtypes [20]. It is well known that the M₃R stimulates IP₃-dependent intracellular Ca²⁺-release ([29,2]. However, like S1P [30], stimulation of M₃R can also activate RhoA-dependent signalling pathways leading to increased myofilament sensitivity of smooth muscle [31,32]. On the other hand, activation of M₂Rs in airway smooth muscle has been shown to increase the sensitivity of myofilaments to Ca²⁺ and to inhibit noradrenaline-induced increases in intracellular cAMP [33,34]. In HEK-293 cells, DLS and DMS markedly reduced both M₂R-and M₃R-mediated increases in [Ca²⁺]_i [5].

In the present study, we therefore also examined which of these two receptor subtypes (M₂R or M₃R) is involved in the SPHK1-dependent constriction of peripheral airways. To address this issue, we carried out a series of functional experiments using PCLS preparations from M₂R-and M₃R-deficient mice (M₂R-KO, M₃R-KO) and their corresponding wild-type controls (M₂R-wt, M₃R-wt). To rule out potential differences in SPHK1 expression between wt and KO animals we initially performed a set of quantitative

RT-PCR studies. These studies showed that inactivation of the M₂R and M₃R genes had no significant effect on the relative expression levels of SPHK1 compared to the corresponding wt controls. Moreover, confocal laser scanning microscopic studies showed that the localization and distribution of SPHK1 protein were similar in all mouse strains. In agreement with the results of a previous study [20], the peripheral airways of M₃R-KO mice showed an about 50 % reduction in the magnitude of the initial muscarine induced constriction response, as compared to the corresponding response obtained with preparations from M₃R-wt mice. We previously demonstrated that the bronchoconstrictor response remaining in the M₃R-KO mice is exclusively mediated by M₂Rs [20].

Changes in [Ca²⁺]_i are the main trigger in the initiation of MR-mediated bronchoconstriction. The initial phase of constriction of intraparenchymal airways is known to be mediated partly via release of Ca²⁺ from intracellular stores, as shown by the presence of this phase under blockade of ion influx by La³⁺ or SKF96365. The considerable reduction of the initial constriction by La³⁺ or SKF96365 further indicates that influx of Ca²⁺ is also part of this phase of muscarine-mediated constriction. We defined the bronchoconstriction in response to muscarine as 100 % and analyzed the inhibition under various experimental conditions. Blockade of SPHK1 by either DHS or DMS almost completely abolished the initial phase of constriction in bronchi from M₃R-KO mice (Fig. 5 Tab. 2). In contrast, DHS or DMS only partially reduced this early response in bronchi from M₂R-KO and wt-mice

**Figure 4**

Effect of various treatments on muscarine-mediated reductions in luminal area of peripheral bronchi from FVB mice. The luminal area of peripheral bronchi (expressed in %) was recorded by videomorphometry after application of 10^{-6} M muscarine alone or after application of 10^{-6} M muscarine in the presence of (A) 10^{-6} M La^{3+} (7 slices from 4 lungs), (B) SKF 96365 (SKF 10^{-5} M, 9 slices from 4 lungs), (C) 10^{-6} M La^{3+} in combination with 10^{-6} M DHS (7 slices from 4 lungs), or (D) 10^{-5} M SKF 96365 in combination with 10^{-6} M DHS (8 slices from 4 lungs). Data are given as means \pm S.E.M. E-F) Summary of effects of various treatments on muscarine-mediated reductions in luminal area of peripheral bronchi from FVB mice. Luminal area (expressed in %) determined 1 min (initial contraction, E) and 15 min (sustained contraction, G) after application of 10^{-6} M muscarine alone or of muscarine in combination with either La^{3+} (both 10^{-6} M) or La^{3+} in combination with DHS or DMS (both 10^{-8} M). Luminal area (expressed in %) determined 1 min (initial contraction, F) and 15 min (sustained contraction, H) after application of muscarine alone or of muscarine in combination with either SKF 96365 (10^{-5} M) or SKF 96365 in combination with 10^{-8} M DHS or DMS. Asterisks indicate $p < 0.05$ for the comparison with application of muscarine alone (E-F). Daggers indicate $p < 0.05$ for the comparison with application of muscarine in combination with La^{3+} (E, G). Data are given as means \pm S.E.M.

Table 3: Effects of DHS and DMS on muscarine-induced reductions in luminal airway area in PCLS from M₂ R-KO and their corresponding wild-type mice. The number of experiments (lungs/slices), mean airway diameter in μm , and the muscarine-induced constriction in luminal airway area (expressed in %) determined after 1 min (1) and 15 min (2) after stimulation with muscarine and 1 min (3) and 15 min (4) after stimulation with muscarine in combination with DHS or DMS (both 10^{-6} M or 10^{-8} M) are shown. In all experiments, the muscarine concentration was 10^{-6} M. The initial phase (1 vs 3) and the sustained phase (2 vs 4) of constriction were reduced in the presence of DHS or DMS. Data are given as means \pm S.E.M.

M ₂ R-wt Lungs /slices	Diameter [μm]	Area [%] 1	Area [%] 2	Area [%] 3	Area [%] 4	p (1 vs. 3)	p (2 vs. 4)
6/7	208 \pm 9	Mus 35 \pm 9	32 \pm 9	Mus/DHS 10^{-6} M 77 \pm 11	52 \pm 11	p \leq 0.05	p \leq 0.05
7/8	213 \pm 8	Mus 46 \pm 6	45 \pm 12	Mus/DHS 10^{-8} M 61 \pm 9	60 \pm 9	n.s. p = 0.078	p \leq 0.05
5/5	202 \pm 17	Mus 40 \pm 10	42 \pm 9	Mus/DMS 10^{-6} M 72 \pm 9	66 \pm 10	p \leq 0.05	p \leq 0.05
7/7	217 \pm 8	Mus 54 \pm 10	41 \pm 9	Mus/DMS 10^{-8} M 69 \pm 10	60 \pm 10	p \leq 0.05	p \leq 0.05
M ₂ R-KO							
6/6	210 \pm 8	Mus 50 \pm 11	54 \pm 11	Mus/DHS 10^{-6} M 79 \pm 7	82 \pm 7	p \leq 0.05	p \leq 0.05
7/7	194 \pm 9	Mus 44 \pm 10	48 \pm 8	Mus/DHS 10^{-8} M 74 \pm 8	74 \pm 7	p \leq 0.05	p \leq 0.05
7/8	218 \pm 8	Mus 56 \pm 8	62 \pm 7	Mus/DMS 10^{-6} M 83 \pm 6	79 \pm 6	p \leq 0.05	p \leq 0.05
7/7	189 \pm 9	Mus 43 \pm 13	51 \pm 11	Mus/DMS 10^{-8} M 71 \pm 9	73 \pm 9	p \leq 0.05	p \leq 0.05

(Fig. 5). This observation strongly suggests that stimulation of M₂R_s mediates activation of SPHK1, which eventually triggers the release of Ca²⁺ from intracellular stores leading to bronchoconstriction. The role of M₂R in airway smooth muscle contraction appears multi-functional in that the receptor can modulate the function of smooth muscle by activation of multiple signalling pathways including tyrosine kinase activation and stimulation/inhibition of ion channels [35,32]. Phosphorylation of myosin light chain and activation of PKC play important roles in the maintenance of smooth muscle contractions [36,37]. Since S1P has been shown to stimulate myosin phosphorylation [8,38], it is likely that this response is also mediated by the M₂R subtype.

Our findings strongly suggest that SPHK1 activation is part of the signalling response to M₂R stimulation in peripheral mouse airways. These airways resemble in their structure and composition of cell types human distal airways [39]. Like human distal airways, murine peripheral airways about 200 μm in diameter that are terminal bronchioles lack submucosal glands, cartilage and contain smooth muscle and Clara cells, in addition to ciliated cells [39]. In studies using monkey and rat peripheral airways, the ACh analogue methacholine (MCh) induced similar responses in large and small mammals [40]. It is therefore likely that the distal airways of man and mice, both of which are also MCh-sensitive [17], share similar MR signalling pathways. In addition, it has been shown that

human airway smooth muscle cells constrict in response to S1P [7,8], suggesting that the MR-SPHK1-S1P signalling pathway is also present in human peripheral airways.

Conclusion

In conclusion, in this study we demonstrated the existence of a novel signalling pathway in the regulation of peripheral airways. We found that MR-mediated constriction of murine peripheral airways is mediated, in part, by activation of SPHK. Our data suggest that muscarinic activation of SPHK contributes to the initial and sustained phase of constriction. The SPHK activation in the initial phase is mainly mediated via the M₂R subtype. These findings could be of relevance for the development of novel drugs useful for the treatment of chronic obstructive pulmonary disease and asthma. For example, one may speculate that altered S1P signalling may contribute to the hyperreactivity of peripheral airways under pathological conditions.

List of abbreviations

ACh acetylcholine

CT threshold cycle

MR muscarinic acetylcholine receptor

wt wild-type control

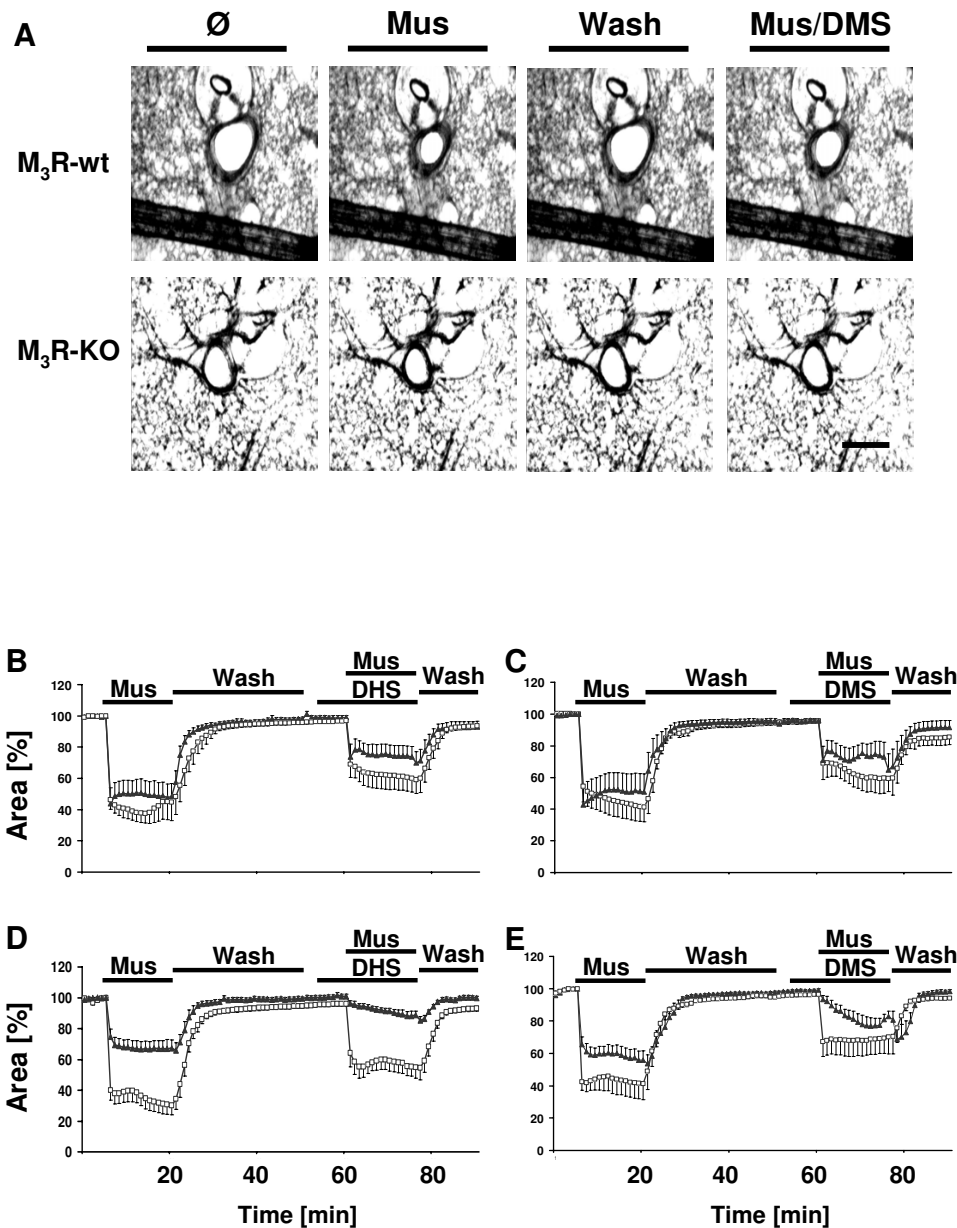


Figure 5

Muscarine-mediated changes in luminal area of peripheral bronchi from wild-type and MR deficient mice. Changes in luminal area of mouse peripheral airways were recorded by videomorphometry after cumulative application of different concentrations of muscarine. (A) Videomorphometric images of precision cut lung slices before (\emptyset), 1 min after stimulation with muscarine (10^{-6} M), after 15 min wash out (Wash) and 1 min after stimulation with muscarine in presence of DMS (10^{-8} M). The bronchi from wild-type (M_3R -wt) and M_3R -KO mice constricted in response to 10^{-6} M muscarine. In M_3R -wt mice, the constriction was slightly reduced in presence of DMS but abolished in M_3R -KO mice. Bar = 200 μ m. (B-D) Effect of DHS and DMS on muscarine-mediated reductions in luminal area of murine peripheral bronchi in the absence of the M_2R or M_3R subtypes. (B-C) Luminal area of peripheral airways from M_2R -KO (triangles) and M_2R -wt mice (squares) (expressed in % in response to application of 10^{-6} M muscarine (Mus) alone or after application of muscarine (10^{-6} M) in combination with DHS (B) or DMS (C) (both 10^{-8} M). Both DHS and DMS significantly inhibited the muscarine-induced constriction in airways of both M_2R -KO and M_2R -wt mice. (D, E) Luminal area of peripheral airways (expressed in %) from M_3R -KO (triangles) and M_3R -wt (squares) mice in response to application of 10^{-6} M muscarine alone or after application of muscarine (10^{-6} M) in combination with DHS (D) or DMS (E) (both 10^{-8} M). Both DHS and DMS significantly inhibited the muscarine-induced constriction in airways of both M_3R -KO and M_3R -wt mice. Data are given as means \pm S.E.M.

Table 4: Effects of DHS and DMS on muscarine-induced reductions in luminal airway area in PCLS from M₃ R-KO and their corresponding wild-type mice. The number of experiments (lungs/slices), mean airway diameter in μm , and the muscarine-induced constriction in luminal airway area (expressed in %) determined after 1 min (1) and 15 min (2) after stimulation with muscarine and 1 min (3) and 15 min (4) after stimulation with muscarine in combination with DHS or DMS (both 10^{-6} M or 10^{-8} M) are shown. In all experiments, the muscarine concentration was 10^{-6} M. The initial phase (1 vs 3) and the sustained phase (2 vs 4) of constriction were reduced in presence of DHS or DMS. Data are given as means \pm S.E.M.

M ₃ R-wt Lungs /slices	Diameter [μm]	Area [%] 1	Area [%] 2	Area [%] 3	Area [%] 4	p (1 vs. 3)	p (2 vs. 4)
6/6	221 \pm 10	Mus 53 \pm 7	47 \pm 8	Mus/DHS 10^{-6} M 75 \pm 7	69 \pm 11	n.s.	p \leq 0.05
8/9	204 \pm 10	Mus 40 \pm 6	30 \pm 6	Mus/DHS 10^{-8} M 64 \pm 9	55 \pm 6	p \leq 0.05	p \leq 0.01
6/7	203 \pm 6	Mus 41 \pm 10	37 \pm 8	Mus/DMS 10^{-6} M 64 \pm 10	56 \pm 8	p \leq 0.05	p \leq 0.05
5/6	197 \pm 8	Mus 42 \pm 5	41 \pm 10	Mus/DMS 10^{-8} M 71 \pm 7	69 \pm 9	p \leq 0.05	p \leq 0.05
M ₃ R-KO 4/4	205 \pm 18	Mus 69 \pm 2	51 \pm 4	Mus/DHS 10^{-6} M 77 \pm 8	62 \pm 12	n.s.	n.s.
8/9	188 \pm 9	Mus 75 \pm 6	67 \pm 6	Mus/DHS 10^{-8} M 96 \pm 2	88 \pm 4	p \leq 0.05	p \leq 0.05
7/7	202 \pm 12	Mus 75 \pm 4	67 \pm 6	Mus/DMS 10^{-6} M 97 \pm 1	82 \pm 4	p \leq 0.05	p \leq 0.05
9/9	196 \pm 7	Mus 65 \pm 5	56 \pm 6	Mus/DMS 10^{-8} M 93 \pm 2	81 \pm 3	p \leq 0.01	p \leq 0.05

M₂R-KO muscarinic acetylcholine receptor 2-deficient mice

M₃R-KO muscarinic acetylcholine receptor 3-deficient mice

PLC β phospholipase C beta

PCLS Precision cut lung slices

SKF96365 1-2-(4-methoxyphenyl)-2-[3-(4-methoxyphenyl) propoxy]-ethyl-1H-imidazole

S1P sphingosine 1-phosphate

SPHK sphingosine kinases

IP₃ inositol 1, 4, 5-trisphosphate

DHS D, L-threo-dihydrosphingosine

DMS N, N-dimethyl-sphingosine

NAcS N-acetylsphingosine

MCh Methacholine

Authors' contributions

PM, NP, SA, WS, SW and RVH carried out the videomorphometric experiments and performed qRT-PCR and immunohistochemistry. JW developed the KO-mice and participated together with WK and RVH in writing and preparation of the manuscript and in the statistical analysis. YB was involved in the design of the study and the immunohistochemical investigations. The data presented in the manuscript are part of the doctoral thesis of PM, NP, SA, WS.

Acknowledgements

We thank Ms K. Michael for skilful technical assistance.

References

- Wess J, Blin N, Mutschler E, Bluml K: **Muscarinic acetylcholine receptors: structural basis of ligand binding and G protein coupling.** *Life Sci* 1995, **56(11-12)**:915-922.
- Caulfield MP, Birdsall NJ: **International Union of Pharmacology. XVII. Classification of muscarinic acetylcholine receptors.** *Pharmacol Rev* 1998, **50(2)**:279-290.
- Jacoby DB, Fryer AD: **Anticholinergic therapy for airway diseases.** *Life Sci* 2001, **68(22-23)**:2565-2572.
- Meyer zu Heringdorf D, Lass H, Alemany R, Laser KT, Neumann E, Zhang C, Schmidt M, Rauen U, Jakobs KH, van Koppen CJ: **Sphingosine kinase-mediated Ca²⁺ signalling by G-protein-coupled receptors.** *Embo J* 1998, **17(10)**:2830-2837.
- van Koppen CJ, Meyer zu Heringdorf D, Alemany R, Jakobs KH: **Sphingosine kinase-mediated calcium signaling by muscarinic acetylcholine receptors.** *Life Sci* 2001, **68(22-23)**:2535-2540.
- Olivera A, Spiegel S: **Sphingosine kinase: a mediator of vital cellular functions.** *Prostaglandins Other Lipid Mediat* 2001, **64(1-4)**:123-134.

7. Ammit AJ, Hastie AT, Edsall LC, Hoffman RK, Amrani Y, Krymskaya VP, Kane SA, Peters SP, Penn RB, Spiegel S, et al.: **Sphingosine 1-phosphate modulates human airway smooth muscle cell functions that promote inflammation and airway remodeling in asthma.** *Faseb J* 2001, **15(7)**:1212-1214.
8. Rosenfeldt HM, Amrani Y, Watterson KR, Murthy KS, Panettieri RA Jr, Spiegel S: **Sphingosine-1-phosphate stimulates contraction of human airway smooth muscle cells.** *Faseb J* 2003, **17(13)**:1789-1799.
9. Lacasse Y, Brosseau L, Milne S, Martin S, Wong E, Guyatt GH, Goldstein RS: **Pulmonary rehabilitation for chronic obstructive pulmonary disease.** *Cochrane Database Syst Rev* 2002, **(3)**:CD003793.
10. Escolar JD, Escolar MA, Guzman J, Roques M: **Morphological hyperplasia of the small airways.** *Histol Histopathol* 2003, **18(1)**:19-26.
11. Wohlsen A, Uhlig S, Martin C: **Immediate allergic response in small airways.** *Am J Respir Crit Care Med* 2001, **163(6)**:1462-1469.
12. Kohama T, Olivera A, Edsall L, Nagiec MM, Dickson R, Spiegel S: **Molecular cloning and functional characterization of murine sphingosine kinase.** *J Biol Chem* 1998, **273(37)**:23722-23728.
13. Melendez AJ, Carlos-Dias E, Gosink M, Allen JM, Takacs L: **Human sphingosine kinase: molecular cloning, functional characterization and tissue distribution.** *Gene* 2000, **251(1)**:19-26.
14. Fukuda Y, Kihara A, Igarashi Y: **Distribution of sphingosine kinase activity in mouse tissues: contribution of SPHK1.** *Biochem Biophys Res Commun* 2003, **309(1)**:155-160.
15. Liu H, Sugiura M, Nava VE, Edsall LC, Kono K, Poulton S, Miltien S, Kohama T, Spiegel S: **Molecular cloning and functional characterization of a novel mammalian sphingosine kinase type 2 isoform.** *J Biol Chem* 2000, **275(26)**:19513-19520.
16. Young KW, Willets JM, Parkinson MJ, Bartlett P, Spiegel S, Nahorski SR, Challiss RA: **Ca²⁺/calmodulin-dependent translocation of sphingosine kinase: role in plasma membrane relocation but not activation.** *Cell Calcium* 2003, **33(2)**:119-128.
17. Held HD, Martin C, Uhlig S: **Characterization of airway and vascular responses in murine lungs.** *Br J Pharmacol* 1999, **126(5)**:1191-1199.
18. Olivera A, Spiegel S: **Sphingosine-1-phosphate as second messenger in cell proliferation induced by PDGF and FCS mitogens.** *Nature* 1993, **365(6446)**:557-560.
19. Coulson FR, Fryer AD: **Muscarinic acetylcholine receptors and airway diseases.** *Pharmacol Ther* 2003, **98(1)**:59-69.
20. Struckmann N, Schwering S, Wiegand S, Gschnell A, Yamada M, Kummer W, Wess J, Haberberger RV: **Role of muscarinic receptor subtypes in the constriction of peripheral airways: studies on receptor-deficient mice.** *Mol Pharmacol* 2003, **64(6)**:1444-1451.
21. Gomeza J, Shannon H, Kostenis E, Felder C, Zhang L, Brodtkin J, Grinberg A, Sheng H, Wess J: **Pronounced pharmacologic deficits in M2 muscarinic acetylcholine receptor knockout mice.** *Proc Natl Acad Sci U S A* 1999, **96(4)**:1692-1697.
22. Yamada M, Miyakawa T, Duttaroy A, Yamanaka A, Moriguchi T, Makita R, Ogawa M, Chou CJ, Xia B, Crawley JN, et al.: **Mice lacking the M3 muscarinic acetylcholine receptor are hypophagic and lean.** *Nature* 2001, **410(6825)**:207-212.
23. Murate T, Banno Y, K TK, Watanabe K, Mori N, Wada A, Igarashi Y, Takagi A, Kojima T, Asano H, et al.: **Cell type-specific localization of sphingosine kinase 1a in human tissues.** *J Histochem Cytochem* 2001, **49(7)**:845-855.
24. Martin C, Uhlig S, Ullrich V: **Videomicroscopy of methacholine-induced contraction of individual airways in precision-cut lung slices.** *Eur Respir J* 1996, **9(12)**:2479-2487.
25. Martin RJ: **Therapeutic significance of distal airway inflammation in asthma.** *J Allergy Clin Immunol* 2002, **109(2 Suppl)**:S447-460.
26. Hakonarson H, Grunstein MM: **Regulation of second messengers associated with airway smooth muscle contraction and relaxation.** *Am J Respir Crit Care Med* 1998, **158(5 Pt 3)**:S115-122.
27. Murray RK, Kotlikoff MI: **Receptor-activated calcium influx in human airway smooth muscle cells.** *J Physiol* 1991, **435**:123-144.
28. Oonuma H, Nakajima T, Nagata T, Iwasawa K, Wang Y, Hazama H, Morita Y, Yamamoto K, Nagai R, Omata M: **Endothelin-1 is a potent activator of nonselective cation currents in human bronchial smooth muscle cells.** *Am J Respir Cell Mol Biol* 2000, **23(2)**:213-221.
29. Wess J: **Molecular biology of muscarinic acetylcholine receptors.** *Crit Rev Neurobiol* 1996, **10(1)**:69-99.
30. Bolz SS, Vogel L, Sollinger D, Derwand R, Boer C, Pitson SM, Spiegel S, Pohl U: **Sphingosine kinase modulates microvascular tone and myogenic responses through activation of RhoA/Rho kinase.** *Circulation* 2003, **108(3)**:342-347.
31. Murthy KS, Zhou H, Grider JR, Brautigan DL, Eto M, Makhlof GM: **Differential signalling by muscarinic receptors in smooth muscle: m2-mediated inactivation of myosin light chain kinase via Gi3, Cdc42/Rac1 and p21-activated kinase 1 pathway, and m3-mediated MLC20 (20 kDa regulatory light chain of myosin II) phosphorylation via Rho-associated kinase/myosin phosphatase targeting subunit 1 and protein kinase C/CPI-17 pathway.** *Biochem J* 2003, **374(Pt 1)**:145-155.
32. Ehler FJ: **Contractile role of M2 and M3 muscarinic receptors in gastrointestinal, airway and urinary bladder smooth muscle.** *Life Sci* 2003, **74(2-3)**:355-366.
33. Chiba Y, Sakai H, Misawa M: **Characterization of muscarinic receptors in rat bronchial smooth muscle in vitro.** *Res Commun Mol Pathol Pharmacol* 1998, **102(2)**:205-208.
34. Janssen LJ, Wattie J, Lu-Chao H, Tazzeo T: **Muscarinic excitation-contraction coupling mechanisms in tracheal and bronchial smooth muscles.** *J Appl Physiol* 2001, **91(3)**:1142-1151.
35. Togashi H, Emala CW, Hall IP, Hirshman CA: **Carbachol-induced actin reorganization involves Gi activation of Rho in human airway smooth muscle cells.** *Am J Physiol* 1998, **274(5 Pt 1)**:L803-809.
36. Ochsner M: **Ca²⁺ transient, cell volume, and microviscosity of the plasma membrane in smooth muscle.** *Biochem Pharmacol* 1997, **53(12)**:1765-1777.
37. Kai T, Yoshimura H, Jones KA, Warner DO: **Relationship between force and regulatory myosin light chain phosphorylation in airway smooth muscle.** *Am J Physiol Lung Cell Mol Physiol* 2000, **279(1)**:L52-58.
38. Zhou H, Murthy KS: **Distinctive G protein-dependent signaling in smooth muscle by sphingosine 1-phosphate receptors SIP1 and SIP2.** *Am J Physiol Cell Physiol* 2004, **286(5)**:C1130-1138.
39. Parent RA: **Comparative biology of the normal lung.** Volume 1. CRC Press; 1991.
40. Kott KS, Pinkerton KE, Bric JM, Plopper CG, Avadhanam KP, Joad JP: **Methacholine responsiveness of proximal and distal airways of monkeys and rats using videomicrometry.** *J Appl Physiol* 2002, **92(3)**:989-996.

Publish with **BioMed Central** and every scientist can read your work free of charge

"BioMed Central will be the most significant development for disseminating the results of biomedical research in our lifetime."

Sir Paul Nurse, Cancer Research UK

Your research papers will be:

- available free of charge to the entire biomedical community
- peer reviewed and published immediately upon acceptance
- cited in PubMed and archived on PubMed Central
- yours — you keep the copyright

Submit your manuscript here:
http://www.biomedcentral.com/info/publishing_adv.asp

